Electron magnetohydrodynamic turbulence

D. Biskamp, E. Schwarz, and A. Zeiler
Max-Planck-Institut für Plasmaphysik, D-85748 Garching, Germany

A. Celani
Istituto di Cosmogeofisica del CNR, 10133 Torino, Italy

J. F. Drake
Institute for Plasma Research, University of Maryland, College Park, Maryland 20742

(Received 23 September 1998; accepted 17 November 1998)

Electron magnetohydrodynamic (EMHD) turbulence is studied in two- and three-dimensional (2D and 3D) systems. Results in 2D are particularly noteworthy. Energy dissipation rates are found to be independent of the diffusion coefficients. The energy spectrum follows a $k^{-5/3}$ law for $kd_e>1$ and $k^{-7/3}$ for $kd_e<1$, which is consistent with a local spectral energy transfer independent of the linear wave properties, contrary to magnetohydrodynamic (MHD) turbulence, where the Alfvén effect dominates the transfer dynamics. In 3D spectral properties are similar to those in 2D. © *1999 American Institute of Physics.* [S1070-664X(99)00103-2]

I. INTRODUCTION

In many weakly collisional high-β plasmas, spatial scales smaller than the ion inertial length and time scales shorter than the ion cyclotron period can be excited. To account for such phenomena we have to abandon the magnetohydrodynamic (MHD) approximation and resort to a two-fluid description, where in addition to the ion equation of motion we consider the generalized Ohm's law

$$\mathbf{E}=-\frac{1}{c}\mathbf{v}_e\times\mathbf{B}-\frac{1}{en}\nabla p_e-\frac{m_e}{en}(\partial_t n\mathbf{v}_e+\nabla\cdot\mathbf{v}_e\mathbf{v}_e n)+\eta\mathbf{j}-\nu_e\frac{m_e}{e}\nabla^2\mathbf{v}_e. \tag{1}$$

Here it is assumed that collisions are still frequent enough to make the pressure isotropic, and the divergence of the stress tensor is replaced by a scalar viscous diffusion term. The latter assumption is a very coarse approximation because of the strong difference between parallel (to the magnetic field) and perpendicular viscosity in a plasma. Here ν_e is essentially the perpendicular electron viscosity, but the details of the viscous behavior are not important in the present context, where the viscosity serves primarily as an energy sink. If we focus on the small-scale dynamics $l<c/\omega_{pi}$, the ions can be considered as a motionless neutralizing background, such that the electron flow determines the electric current. On insertion of **E** into Faraday's law we obtain a self-consistent nonlinear equation for the magnetic field, which can be written in the form

$$\partial_t\left(\mathbf{B}-\frac{c^2}{\omega_{pe}^2}\nabla^2\mathbf{B}\right)-\nabla\times\left[\mathbf{v}_e\times\left(\mathbf{B}-\frac{c^2}{\omega_{pe}^2}\nabla^2\mathbf{B}\right)\right]=\frac{\eta c^2}{4\pi}\nabla^2\mathbf{B}-\nu_e\frac{c^2}{\omega_{pe}^2}\nabla^2\nabla^2\mathbf{B}, \tag{2}$$

where

$$\mathbf{v}_e=-\frac{1}{en}\mathbf{j}=-\frac{c}{4\pi en}\nabla\times\mathbf{B}. \tag{3}$$

Note that the pressure contribution vanishes on the usual assumption $p_e=p_e(n)$. Equation (2) is called electron magnetohydrodynamics (EMHD), which has attracted considerable attention in recent years. On the one hand, there are the applications to plasma opening switches and *Z* pinches, see, e.g., Ref. 1. Here the mean density gradient plays a crucial role through the term $\nabla(1/n)\times(\mathbf{j}\times\mathbf{B})$ in Eq. (2). On the other hand, special interest in EMHD arises in the field of quasicollisionless magnetic reconnection,[2–5] which is generally believed to be responsible for the fast magnetic energy release in many laboratory and space plasmas, in particular in the geomagnetic tail. In this context the mean density gradient is less important. We therefore assume homogeneous density, which is consistent with the quasineutrality condition $\nabla\cdot\mathbf{j}=0$.

Linearizing (2) about a static equilibrium embedded in a homogeneous field B gives (neglecting dissipation)

$$\omega\left(1+\frac{c^2}{\omega_{pe}^2}\right)\mathbf{B}_1+\frac{cB}{4\pi en}k_\parallel i\mathbf{k}\times\mathbf{B}_1=0, \tag{4}$$

which yields the dispersion relation for the whistler,

$$\omega^2=\frac{c^4}{\omega_{pe}^4}\Omega_e^2\frac{k_\parallel^2k^2}{(1+k^2c^2/\omega_{pe}^2)^2}, \tag{5}$$

$\Omega_e=eB/m_ec$. The whistler is a transverse circularly polarized wave, which rotates about the magnetic field in the sense of the electron cyclotron motion,

$$\mathbf{B}_1=\pm i(\mathbf{k}/k)\times\mathbf{B}_1. \tag{6}$$

It is convenient to cast the EMHD equation into dimensionless form using the whistler time scale $\tau_W=L^2(\omega_{pe}/c)^2/\Omega_e$, a typical field intensity B_0, and a typical spatial scale length L,

$$\partial_t(1-d_e^2\nabla^2)\mathbf{B}-\nabla\times[\mathbf{v}_e\times(1-d_e^2\nabla^2)\mathbf{B}]=\eta_\nu(-\nabla^2)^\nu\mathbf{B}, \quad (7)$$

where $d_e=c/(\omega_{pe}L)$. We have also introduced generalized diffusion terms with $\nu=1$ corresponding to resistivity and $\nu=2$ to (perpendicular) electron viscosity. In numerical studies of turbulence one often uses higher-order diffusion $\nu>2$ in order to separate nondissipative and dissipative scales more clearly.

Reconnection processes are often considered in two-dimensional (2D) approximation. Assuming $\partial_z=0$, the magnetic field and current density can be written in the form

$$\mathbf{B}=\mathbf{e}_z\times\nabla\psi+\mathbf{e}_z(B_{z0}+b), \quad (8)$$

$$\mathbf{j}=\nabla b\times\mathbf{e}_z+\mathbf{e}_z\nabla^2\psi=-\mathbf{v}_e \quad (9)$$

which indicates that the axial field fluctuation b acts as a stream function of the poloidal electron flow. The two-dimensional version of the EMHD equation (7) consists of two equations for ψ and b:

$$\partial_t(\psi-d_e^2 j)+\mathbf{v}_e\cdot\nabla(\psi-d_e^2 j)=\eta_\nu(-\nabla^2)^\nu\psi, \quad (10)$$

$$\partial_t(b-d_e^2 w)+\mathbf{v}_e\cdot\nabla(b-d_e^2 w)+\mathbf{B}\cdot\nabla j=\eta_\nu(-\nabla^2)^\nu b, \quad (11)$$

$$j=\nabla^2\psi, \quad w=\nabla^2 b.$$

[The mean axial field B_{z0} does not appear in (11), which is a consequence of the incompressibility of the electron flow. One should however, keep in mind that a strong axial field will couple the ions to the electrons also on scales $<d_i$ and hence invalidate the EMHD approximation. Hence B_{z0} should not be too large, i.e., we are dealing mainly with high-β plasmas, $\beta\sim 1$.] In 2D linear whistler modes imply a coupling of poloidal and axial field perturbations,

$$b_k=\pm k\psi_k, \quad (12)$$

which is the 2D analog of (6).

Equations (10), (11) are formally similar to the equations of 2D MHD, but are more complicated than the latter because of the intrinsic scale d_e. Hence one has in general to distinguish between the long-wavelength regime $kd_e<1$ and the short-wavelength regime $kd_e>1$. Note that EMHD does not reduce to MHD in the limit $d_e\to 0$. Actually EMHD is only valid on scales $l<d_i=\sqrt{m_i/m_e}d_e$, while MHD refers to macroscopic scales $l>d_i$.

II. IDEAL INVARIANTS

In turbulence theory the ideal invariants of the dynamical equations play an important role. It can easily be checked that neglecting dissipation the EMHD equation (7) conserves the energy

$$E=\frac{1}{2}\int (B^2+d_e^2 j^2)d^3x \quad (13)$$

and the generalized helicity

$$F=\int (\mathbf{A}-d_e^2\mathbf{j})\cdot(\mathbf{B}-d_e^2\nabla^2\mathbf{B})d^3x, \quad (14)$$

$\nabla\times\mathbf{A}=\mathbf{B}$, which for $d_e\to 0$ reduces to the magnetic helicity H and for $d_e\to\infty$ to the (electron) kinetic energy H^V. Expression (14) also contains terms $\propto\int\mathbf{j}\cdot\mathbf{B}d^3x$ reminiscent of the cross-helicity $K=\int\mathbf{v}\cdot\mathbf{B}$ in MHD.

In 2D the ideal equations conserve the following quantities, the energy

$$E=\frac{1}{2}\int\{(\nabla\psi)^2+b^2+d_e^2[j^2+(\nabla b)^2]\}d^2x, \quad (15)$$

the generalized helicity

$$F=\int (b-d_e^2\nabla^2 b)f'(\psi-d_e^2 j)d^2x, \quad (16)$$

and a quantity containing only the electron canonical momentum $p=\psi-d_e^2 j$,

$$G=\int g(\psi-d_e^2 j)d^2x, \quad (17)$$

where f and g are arbitrary functions. Since in turbulence theory the quadratic invariants are most important, the appropriate choice is $f(x)=g(x)=x^2$. Expressions (15)–(17) are generalizations of the corresponding quantities in 2D MHD. As in MHD one expects a direct cascade of the energy and inverse cascades of the helicity F in 3D and the mean square momentum G in 2D. Here we are mainly concerned with processes associated with the direct energy cascade, leaving the investigation of inverse cascades in EMHD to a future study. Though we find that EMHD and MHD turbulence share many properties, which is primarily due to the direct cascade of the energy, there are, however, also distinct differences.

III. 2D EMHD TURBULENCE

Two-dimensional turbulence has previously been considered in various different systems, notably hydrodynamics (see e.g., Refs. 6,7), MHD (e.g., Ref. 8) or Hasegawa-Mima equation (e.g., Refs. 9, 10). These studies are motivated partly by special applications, where the dynamics of the system is quenched in one direction, for instance by a strong magnetic, but partly also because these systems reveal interesting turbulence properties, which are numerically more easily accessible than in fully 3D systems. Also in EMHD first studies that have appeared recently, are concerned with 2D turbulence.[11,12] In this section we therefore focus on 2D EMHD turbulence, which exhibits a number of interesting and unexpected properties, before we discuss the 3D case in Sec. III, which turns out to be rather similar to the 2D behavior.

In addition the numerical simulations discussed in this paper refer only to decaying turbulence. This has the advantage, that in a self-similarly decaying state, which has become independent of the initial conditions, we are dealing only with the intrinsic properties of the turbulence, contrary to forced turbulence, which may reflect particular features of the forcing. On the other hand studies of decaying turbulence may be affected by the lack of stationarity. For instance the

spectral energy flux is not strictly constant in the inertial range, though the variation is small for a sufficiently broad extent of this spectral range.

A. Turbulence generation

At small values of the dissipation coefficients an EMHD system, starting from smooth initial conditions, tends to generate sheet-like structures, which subsequently break up leading to fully developed turbulence. In resistive MHD current sheets of thickness $\delta\sim\eta^{1/2}$ are generated, which are rather stable subject only to tearing instability at high sheet aspect ratio $\Delta/\delta\sim 10^2$,[8] where Δ is the sheet length. The plasma flow v along the sheet is stable owing to the parallel magnetic field generated by the current, which is strong enough $v_A > v$ to suppress the Kelvin-Helmholtz mode.[13] (Originally the term Kelvin-Helmholtz mode refers to the instability of a vortex sheet, i.e., the interface between two regions moving at different velocities. Here we consider the bending instability of a fluid jet, i.e., a vortex double layer.) In an EMHD current sheet conditions are quite different. Here conservation of the canonical momentum $p=\psi-d_e^2 j$, Eq. (10), requires that the magnitude of the axial current density j is limited, $j\sim\psi/d_e^2$, even in much narrower structures $\delta\ll d_e$, such that the poloidal field generated by this current is weak $B\sim\psi\delta/d_e^2$. The poloidal electron flow or current density is of the order of the axial one $\nabla b\sim b/\delta\sim j$, reflecting the whistler property (12). The parallel field is too weak by a factor δ/d_e to stabilize the (electron) Kelvin-Helmholtz mode, which is hence expected to grow for sheets thinner than d_e, where the $\mathbf{B}\cdot\nabla j$ term in (11) becomes small, reducing (11) to the Euler equation for the electron flow. The Kelvin-Helmholtz instability of an EMHD vortex sheet in the absence of a poloidal magnetic field, where Eq. (11) reduces to the Hasegawa-Mima equation, has recently been studied by Bulanov *et al.*[14,15]

The process of turbulence generation is illustrated in Figs. 1a–d. Equations (10) and (11) are solved on a quadratic box of edge size $L=2\pi$ with periodic boundary conditions using a standard pseudospectral method with N^2 modes or collocation points and dealiazing according to the 2/3 rule, hence only $(2/3)^2N^2$ modes are actually advanced. The dissipation terms are integrated exactly. In Fig. 1 we have chosen the smooth initial state

$$\psi(x,y)=\cos(2x+2.3)+\cos(y+4.1), \tag{18}$$

$$b(x,y)=\cos(x+1.4)+\cos(y+0.5), \tag{19}$$

which has been introduced in Ref. 8 as configuration A_1 generalizing the Orszag-Tang vortex, and we use $d_e=1$, $\nu=3$, $\eta_3=10^{-8}$ and $N=1024$. (Results are similar for $\nu=2$, whereas $\nu=1$ corresponding to a pure friction term at high k is in general found to be insufficient to prevent the formation of singularities.) At time $t=2.0$ extended thin sheets have been formed illustrated most clearly in a plot of the ''vorticity'' $w=\nabla^2 b$, Fig. 1a. Subsequently these sheets are disrupted by the onset of instability, Figs. 1b, 1c. In the first phase the dynamics of this instability is identical to the Kelvin-Helmholtz mode of a fluid jet,[13] as becomes clear when rerunning the simulation with $\psi=0$ set at $t=2.0$, which eliminates the small term $\mathbf{B}\cdot\nabla j$ and thus reduces (11) essentially to the Euler equation. At later times the dynamics is, however, different in both cases. While the Kelvin-Helmholtz instability of the Euler system only leads to a set of isolated weakly interacting vortices well-known from 2D hydrodynamic turbulence, Fig. 2, the EMHD system remains in a strongly turbulent state consisting of vortices and microfilaments, Fig. 1c. The latter are constantly regenerated by the small term $\mathbf{B}\cdot\nabla j$, which then break up again into vortices, thus maintaining the turbulent dynamics. Figure 1d illustrates the canonical momentum p at $t=4$, which exhibits the characteristic features of a purely convected quantity, $p=\psi-d_e^2 j\simeq -d_e^2 j$, since ψ is a smooth function.

B. Turbulent energy dissipation

The small-scale turbulent eddies give rise to efficient energy dissipation

$$\frac{dE}{dt}=-\eta_3\int d^2x[(\nabla^2 j)^2+(\nabla w)^2]=-\epsilon. \tag{20}$$

The energy dissipation rate ϵ increases from the very low level in the smooth initial state to a maximum, where turbulence is fully developed, and subsequently decays in a self-similar way. An important result is, that $\epsilon(t)$ is independent of the value of the dissipation coefficient, as shown in Fig. 3, where the time evolution of ϵ is plotted for different values of η_3. Here we start from ''random'' initial conditions called *B*-type in Ref. 8,

$$\psi_{\mathbf{k}}=\exp(-k^2/2k_0^2+2\pi i\alpha_{\mathbf{k}}), \tag{21}$$

$$b_{\mathbf{k}}=\exp(-k^2/2k_0^2+2\pi i\beta_{\mathbf{k}}), \tag{22}$$

where $k^2=k_x^2+k_y^2$, $k_{x,y}=\pm1,\pm2,\ldots$, $\alpha_{\mathbf{k}},\beta_{\mathbf{k}}$ are random phases, and the dominant initial wave number is $k_0=5$. Figure 3a refers to relatively large $d_e=0.3$. Shown are three cases, $\eta_3=10^{-8}$ (dashed line), 10^{-9} (dashed-dotted), and a case starting with 10^{-8}, switching to 10^{-9} at $t=0.5$ and to 10^{-10} at $t=1$ (solid). On reducing the dissipation coefficient the system responds by exciting smaller spatial scales, so that the dissipation rate soon reaches the previous level after a weak overshoot. Figure 3b gives similar plots for a smaller value $d_e=0.033$. Here the dashed curve corresponds to $\eta_3=10^{-8}$, while in the solid line η_3 is switched to 10^{-9} at $t=0.5$ and to 10^{-10} at $t=1$. At $t=1.4$ η_3 is switched down further to 10^{-11} (dashed-dotted). This behavior of the energy dissipation rate is similar in 2D MHD turbulence.[8]

The energy dissipation rate does, however, depend on d_e as is obvious by comparing Figs. 3a and 3b. We find $\epsilon(t)\simeq-(1/d_e)\dot{E}_0(t/d_e)$, i.e., $E(t)=E_0(t/d_e)$. This behavior can be seen from Eqs. (10), (11). Since the term $\mathbf{B}\cdot\nabla j$ in (11) is responsible for the energy transfer giving rise to the direct energy cascade as discussed above, we have approximately

$$\frac{d}{d(t/d_e)}\int_0^k E_k dk\simeq -d_e\int_0^k[\mathbf{B}\cdot\nabla j]_k dk.$$

Figure 3b also suggests that $E(t)$ decays as a power law, roughly $E\sim t^{-1}$, which is similar to the energy decay law in

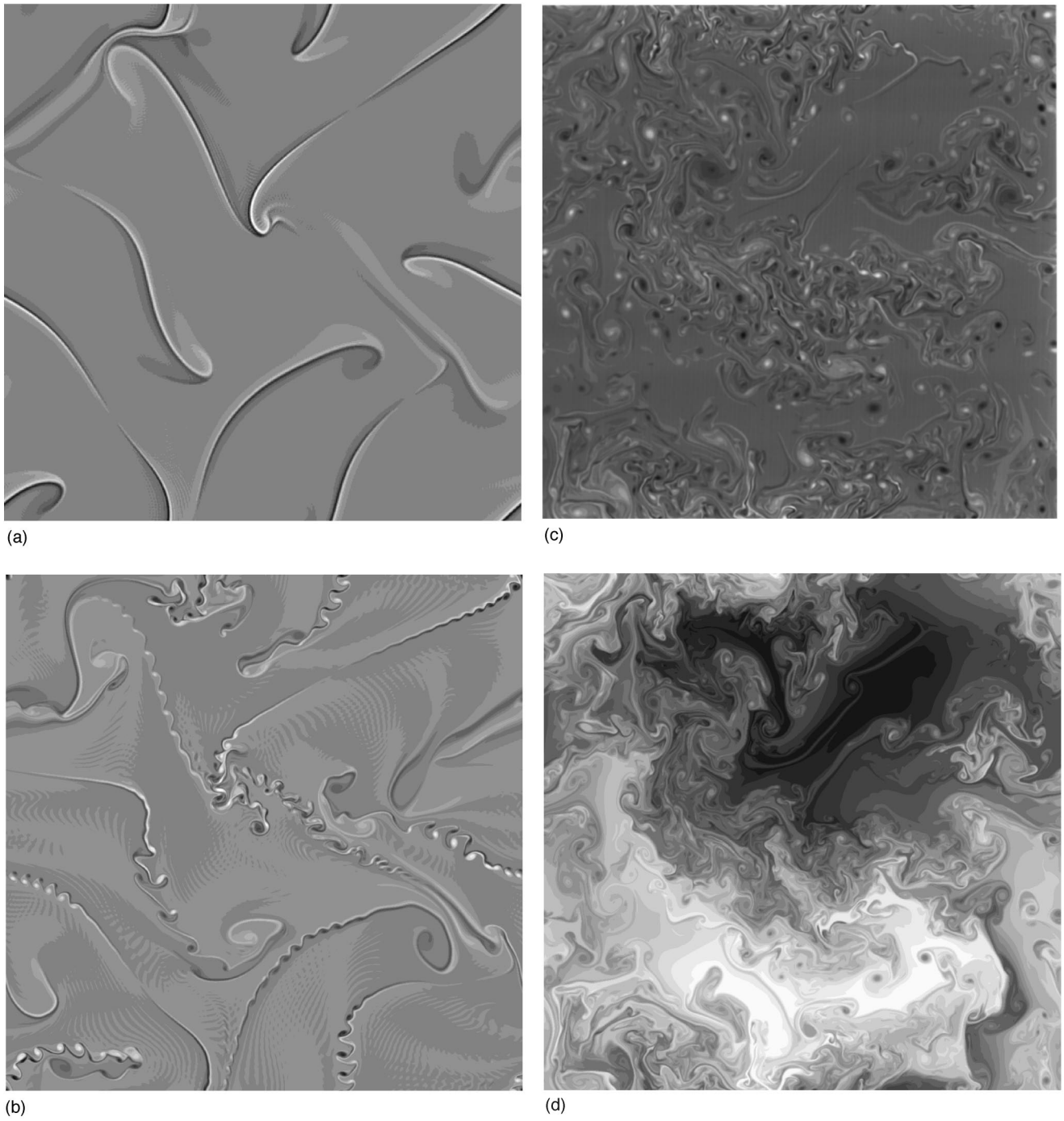

FIG. 1. Generation of small-scale turbulence by the Kelvin-Helmholtz instability. Plots of $w(x,y)$ at $t=2.0$ (a); $t=2.4$ (b); $t=4$ (c). $p(x,y)=\psi-d_e^2 j$ at $t=4$.

2D MHD turbulence.[8] We can, however, not exclude a dependence on the initial conditions as discussed in Ref. 16.

The self-similarity of the decaying turbulence also shows up in the constancy of the ratio of certain macroscopic quantities. Figure 4 displays the time development of the ratios of the axial and poloidal kinetic energies $R_j=\langle j_z^2\rangle/\langle j_p^2\rangle$, where $j_p^2=(\nabla b)^2$, and of the corresponding field energies $R_B=\langle(\nabla\psi)^2\rangle/\langle b^2\rangle$. The simulations give the values $R_j\simeq 1.5$ and $R_B\simeq 3$, independently of d_e. These results reflect the linear whistler property (12), which remains qualitatively valid also in the nonlinear regime.

C. Energy spectrum

A characteristic statistical quantity of a turbulent system is the energy spectrum, which for isotropic turbulence is conveniently considered in the angle-integrated form $E_k, \int E_k dk = E$. While 3D hydrodynamic turbulence exhibits the spectrum $E_k \propto k^{-5/3}$, the famous Kolmogorov law, entrophy conservation in 2D enforces an inverse energy cascade which leads to a much steeper spectrum $E_k \propto k^{-\mu}$, $\mu > 3$. In MHD turbulence energy transfer is different because of the Alfvén effect.[17,18] The magnetic field in the large energy-

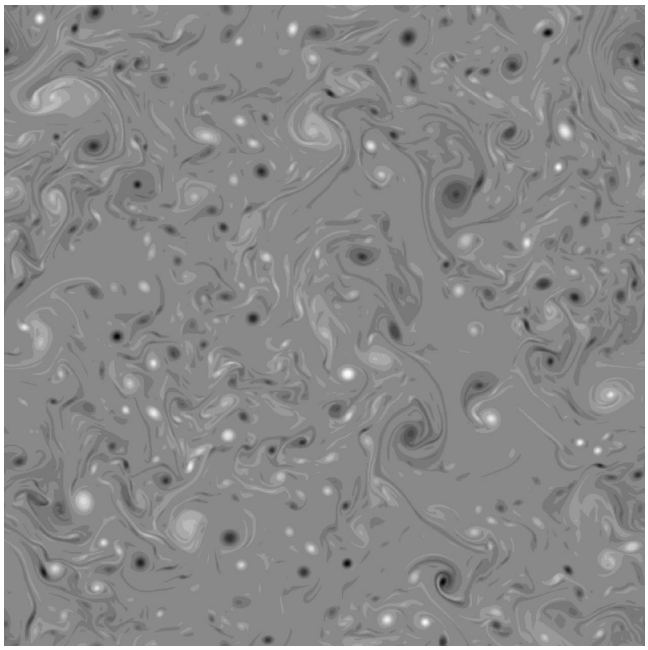

FIG. 2. $w(x,y)$ at $t=5$ from the simulation shown in Fig. 1, but with $\psi=0$ set at $t=4$.

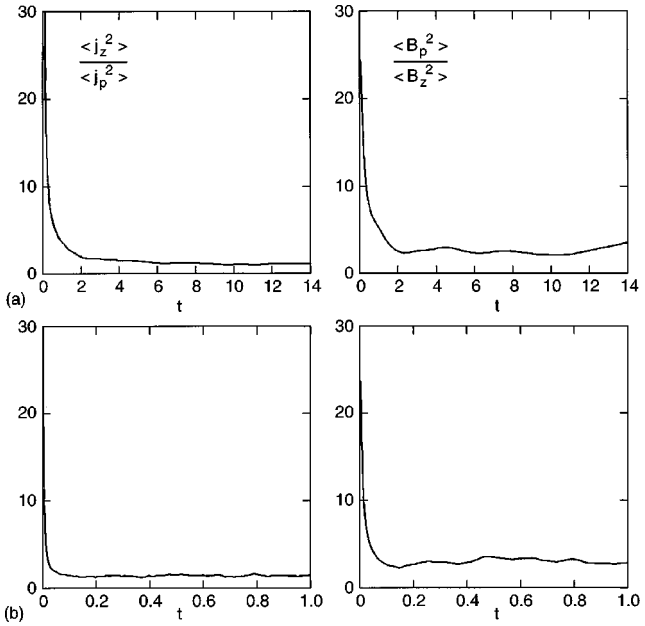

FIG. 4. Time evolution of the ratios of kinetic and magnetic energies for two runs with (a) $d_e=0.3$ and (b) $d_e=0.01$.

containing eddies acts as a guide field on small-scale fluctuations, which behave as Alfvén waves propagating along the large-scale field. Since only oppositely propagating wave packets interact, the interaction time is the Alfvén time $\tau_A=l/v_A$, which is much shorter than the hydrodynamic scrambling time $\tau_l=l/v_l$, where v_l is the velocity fluctuation amplitude at scale l. Hence the spectral energy transfer rate is reduced, which should lead to a flatter energy spectrum, $E_k\propto k^{-3/2}$. This so-called Iroshnikov-Kraichnan spectrum is indeed found in 2D numerical simulations. (Observations of MHD turbulence in the solar wind give a more complex picture.)

In EMHD turbulence the linear perturbations are whistlers propagating along the large-scale magnetic field, which could give rise to a ''whistler effect'' analogous to the Alfvén effect in MHD. However, contrary to Alfvén waves, the whistler is dispersive with high group velocity $v_g\propto k$ for $kd_e<1$ and small group velocity $v_g\simeq 0$ for $kd_e>1$ as seen from the dispersion relation (5). Because of these properties EMHD cannot be written in terms of the whistler variables $b_k\pm k\psi_k$ as can be done in MHD by introducing the Elsaesser variables $v\pm B$. Hence it is an interesting question, whether in EMHD whistler propagation produces a similar correction to the energy spectrum as does the Alfvén effect in MHD.

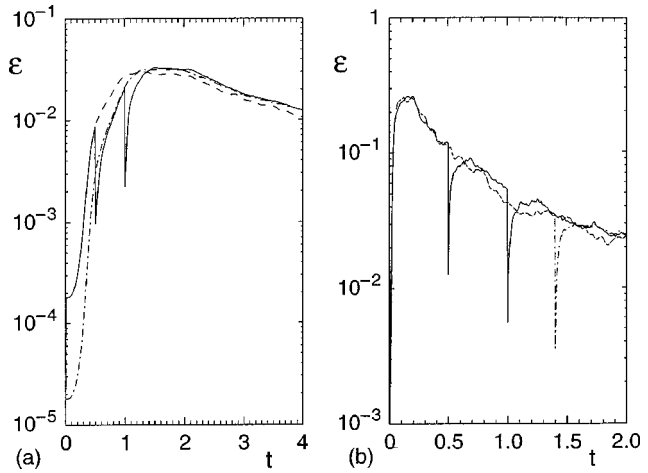

FIG. 3. Energy dissipation rate $\epsilon=-dE/dt$ from simulations with (a) $d_e=0.3$; (b) $d_e=0.033$, for various values of the dissipation coefficient η_3.

We have to distinguish between the different ranges $kd_e>1$ and $kd_e<1$. In the former range numerical simulations reveal an almost exact Kolmogorov spectrum as shown in Fig. 5a. Evaluating different turbulent states we obtain

$$E_k=C\epsilon^{2/3}k^{-5/3} \quad \text{for } kd_e>1, \tag{23}$$

where $C=1.8\pm 0.1$. Since in this range time scales associated with the whistler interaction become longer than the nonlinear eddy scrambling time, the Kolmogorov energy transfer process should dominate leading to the spectrum (23). It is worth noting that this spectral law is found to be valid over the entire range $kd_e>1$ and not only asymptotically for $kd_e\gg 1$. We will come back to this point below.

In the opposite case $kd_e<1$ the character of the turbulence is different, structures resembling those in MHD with current sheets mainly aligned along the magnetic field. Since small-scale structures are less pronounced, a steeper energy spectrum can be expected. This is indeed observed, Fig. 5b:

$$E_k\propto k^{-\mu}, \quad \mu=2.25\pm 0.1 \quad \text{for } kd_e<1. \tag{24}$$

Let us compare this finding with theoretical predictions. Neglecting linear mode propagation effects, i.e., a possible whistler effect, we apply a Kolmogorov-type argument. The

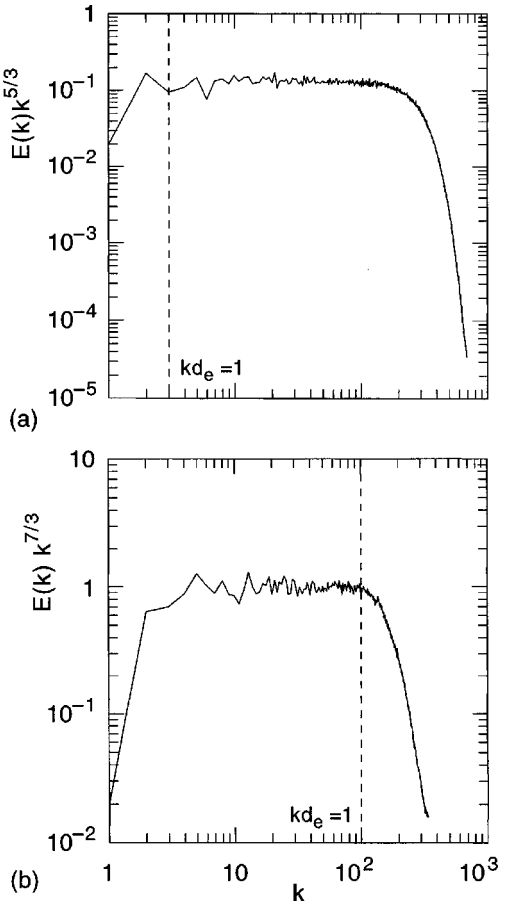

FIG. 5. Compensated plots of the energy spectrum. (a) $k^{5/3}E_k$ for $d_e=0.3$; (b) $k^{7/3}E_k$ for $d_e=0.01$.

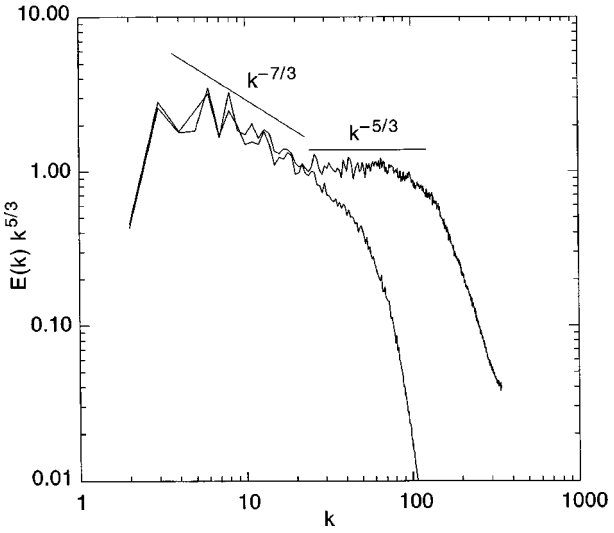

FIG. 6. Compensated energy spectrum $k^{5/3}E_k$ from two runs with $d_e=0.02$. (a) for $\eta_3=10^{-9}$ the spectrum remains within the $k^{-7/3}$ regime; (b) for $\eta_3=10^{-11}$ the large-k part extends into the $k^{-5/3}$ regime with the crossover occurring at $kd_e\simeq 0.5$.

interaction time for eddies of scale l is $\tau_l=l/v_l\sim l^2/b_l$. Hence the energy transfer rate, which is constant in the inertial range, becomes

$$\epsilon\sim E_l/\tau_l\sim b_l^3/l^2,$$

i.e., $b_l^2\sim\epsilon^{2/3}l^{4/3}$ and therefore

$$E_k=k^2|\psi_k|^2+|b_k|^2\sim|b_k|^2\sim lb_l^2\sim\epsilon^{2/3}k^{-7/3}, \tag{25}$$

using $k\sim l^{-1}$. By contrast, if the whistler effect would dominate the dynamics in a way the Alfvén effect does in MHD turbulence, the energy transfer consisting of many weak encounters of oppositely traveling wave packets would be reduced leading to a flatter spectrum, which can be estimated by the following argument. The whistler interaction time is $\tau_W\sim l/v_g(l)\sim l^2/(d_e^2\Omega_e)$. During this time the change of energy is $\delta E_l\sim b_l^2\tau_W/\tau_l$. Because of the random nature of this process the energy transfer time is rather long,

$$\tau_E\sim(E_l/\delta E_l)^2\tau_l\sim\tau_l^2/\tau_W\sim d_e^2\Omega_e l^2/b_l^2.$$

From $\epsilon\sim b_l^2/\tau_E$ we thus obtain

$$E_k\sim(\epsilon d_e^2\Omega_e)^{1/2}k^{-2}. \tag{26}$$

The simulation result clearly favors the $k^{-7/3}$ law, which indicates that even for $kd_e<1$, where wave propagation effects are strong, they do not dominate the spectral transfer process, though they are sufficient to establish equipartition of poloidal and axial field energies $k^2|\psi|^2\simeq|b_k|^2$ in this range.

It is interesting to note that the transition between the two spectral ranges is rather sharp, as demonstrated in Fig. 6. Here the energy spectrum for a case with $d_e=0.02$ is plotted for two values of η_3. While for the higher dissipation $\eta_3=10^{-9}$ the spectrum remains within the $k^{-7/3}$ regime, for lower dissipation $\eta_3=10^{-11}$ it extends into the $k^{-5/3}$ regime, where the rather abrupt crossover occurs at $kd_e\simeq 0.5$. This behavior is caused by the Kelvin-Helmholtz instability, which sets in, when the dissipation scale becomes smaller than d_e. Figure 7 illustrates the turbulence in such a system. The large- and medium-scale structures represent the dynamics when electron inertia can be ignored, while at the small scales the effect of the Kelvin-Helmholtz instability is clearly discernable.

IV. 3D EMHD TURBULENCE

The 2D approximation considered in the previous section is only justified, if the axial field B_{z0} is large enough to suppress Kelvin-Helmholtz instability by the current j_z in the third direction. In the absence of a mean field the turbulence becomes genuinely three-dimensional. Such behavior has recently been studied in 3D simulations of magnetic reconnection in the framework of EMHD.[19] It has been found that Kelvin-Helmholtz instability is excited more readily in z direction than in the poloidal plane leading to a three-dimensional turbulent behavior. Though the reconnection is not faster than in the laminar case, since already in the latter the reconnection rate is fast, independent of the electron inertia depending only on the large-scale configuration, the energy dissipation (=electron heating), which is very weak in the laminar state, becomes large and independent of the microphysics.

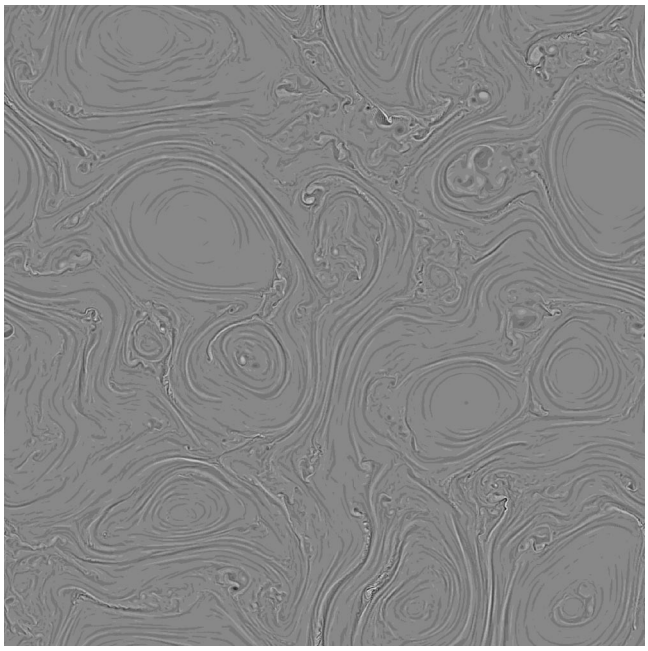

FIG. 7. Plot of $w(x,y)$ for $d_e=0.02$, $\eta_3=10^{-11}$, illustrating the coexistence of both $kd_e<1$ and $kd_e>1$ turbulent structures.

Here we consider the case of 3D homogeneous turbulence analogous to the 2D studies presented in Sec. II. Equation (7) is solved on a cubical box with periodic boundary conditions using a similar numerical scheme as in the 2D simulations. Again we first consider the inertia-dominated regime $kd_e>1$. Here (7) reduces to the 3D Navier-Stokes equation for the electron flow written in the vorticity form, $\nabla\times\mathbf{v}_e=\nabla^2\mathbf{B}$. Contrary to the 2D case, where the small $\mathbf{B}\cdot\nabla j$ term had a strong influence on the dynamics generating a direct energy cascade instead of the inverse one in the 2D Navier-Stokes turbulence, the small terms, i.e., those not multiplied by d_e^2 have little effect in this range. Hence the turbulence has the characteristics of 3D Navier-Stokes turbulence, spatial structures are found to be very similar. Also the energy spectrum is expected to follow the Kolmogorov law (23). Because of the short wave number range available in 3D turbulence simulations a direct verification of the spectral law is difficult. Figure 8a shows the spectrum obtained from a simulation run with $N^3=256^3$ modes and $\nu=3$, where the straight line indicates the Kolmogorov law. For a more quantitative comparison we have plotted the local spectral exponent $\mu(k)=-d\ln E_k/d\ln k$ in the inset with the dashed line at 5/3. Only locally at $kd_e\sim4$ the exponent comes close to the theoretical value. At larger k the spectrum is dominated by the bottleneck effect well-known from 3D simulations of Navier-Stokes turbulence, see e.g., Ref. 20, the local enhancement of the spectrum above the inertial range power law, which is the more pronounced the more abrupt the transition from the inertial range to the dissipation range, i.e., the higher the order of the diffusion operator ν. (In 2D the bottleneck effect is in general much weaker than in 3D. There is no indication of such a hump in the spectra shown in Fig. 5. However, recent studies using still higher spatial resolution[21] show that also in 2D a bottleneck effect appears,

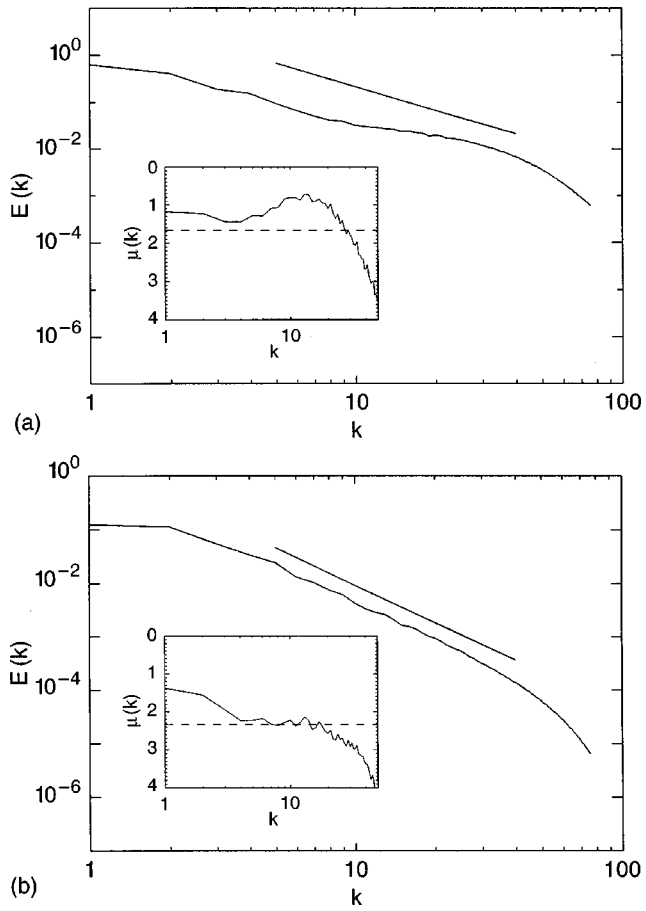

FIG. 8. Energy spectrum of 3D EMHD turbulence. (a) $d_e=1$. The straight line indicates the Kolmogorov spectrum $k^{-5/3}$, the insert gives the local spectral exponent $\mu(k)=-d\ln E_k/d\ln k$. (b) $d_e=0.02$. The straight line indicates the spectrum $k^{-7/3}$.

which is nonlocal contrary to the 3D behavior, and may hence blur the spectral law at high Reynolds numbers.)

In the long-wavelength regime $kd_e<1$ EMHD is differs distinctly from the Navier-Stokes theory, and it is interesting to see, whether the 2D spectral behavior $\sim k^{-7.3}$ persists in 3D. Figure 8b gives the energy spectrum from a simulation run with $d_e=0.02$, $\nu=3$ and again $N^3=256^3$, the straight line and the dashed line in the insert indicating the 7/3 law. As seen from the figure the spectrum follows this law surprisingly well. Hence we find that the spectral properties in 2D and 3D EMHD turbulence are very similar.

V. CONCLUSIONS

We have discussed some important properties of EMHD turbulence, which arises in high-β plasmas at sufficiently low collisionality. Contrary to ordinary MHD, which describes the global dynamics of a plasma on scales $l>c/\omega_{pi}$, EMHD refers to fast small-scale processes $l<c/\omega_{pi}$, where the ions can be considered infinitely heavy, such that the electron flow determines the electric current density. As in MHD the existence of several ideal invariants implies the presence of both direct and inverse cascade processes, where the energy follows a direct cascade both in 2D and 3D. We have further investigated the behavior of 2D and

3D EMHD systems using numerical simulation focusing on freely decaying turbulence. Whereas in MHD turbulence is generated or at least intensified by the tearing instability of current sheets, in EMHD small-scale turbulence arises because of the Kelvin-Helmholtz instability of the strongly sheared electron flows in the current sheets. 2D EMHD properties are most notable. Turbulent energy dissipation rates are found to be independent of the value of the diffusion coefficient, a property already encountered in 2D MHD, which is connected with the direct cascade of the energy. The spectral energy transfer process is, however, different. Though there is a linear mode, the whistler, propagating along the magnetic field, it does not dominate the transfer dynamics, contrary to the Alfvén effect in MHD. The spectral transfer seems to be local giving rise to a 5/3 Kolmogorov spectrum for small scales $kd_e>1$, and a somewhat steeper 7/3 spectrum for long wavelengths $kd_e<1$. The crossover occurs at $kd_e\simeq 0.5$ and is found to be rather abrupt, which is caused by the onset of Kelvin-Helmholtz instability as soon as scales drop below d_e.

Fully three-dimensional EMHD turbulence, which is expected to arise in the absence of a mean magnetic field, exhibits the same spectral characteristics as 2D turbulence, in particular the 7/3 spectrum in the range $kd_e<1$. For short wavelength $kd_e>1$ EMHD reduces to the Navier-Stokes equation. While in the 2D case the weak additional terms play an important role causing the direct energy cascade by violating the entrophy invariance, which is the origin of the inverse energy cascade in 2D Navier-Stokes theory, in 3D EMHD and Navier-Stokes are rather similar at small scales. However, the Kolmogorov law is only marginally verified in the 3D simulations, since because of the short extent of the inertial range the spectrum is dominated by the bottleneck effect, well-known from 3D hydrodynamic turbulence simulations. We have not considered inverse cascade processes arising in EMHD, a topic left to future investigations.

[1] A. S. Kingsep, K. V. Chukbar, and V. V. Yan'kov, in *Reviews of Plasma Physics* (Consultants Bureau, New York, 1990), Vol. 16.
[2] S. V. Bulanov, F. Pegoraro, and A. S. Sakharov, Phys. Fluids B **4**, 2499 (1992).
[3] M. E. Mandt, R. E. Denton, and J. F. Drake, Geophys. Res. Lett. **21**, 73 (1994).
[4] D. Biskamp, E. Schwarz, and J. F. Drake, Phys. Rev. Lett. **75**, 3850 (1995).
[5] K. Avinash, S. V. Bulanov, T. Esirkepov, P. Kaw, F. Pegoraro, P. S. Sasorov, and A. Sen, Phys. Plasmas **5**, 2849 (1998).
[6] M. Brachet, M. Meneguzzi, H. Politano, and P. Sulem, J. Fluid Mech. **194**, 333 (1988).
[7] L. M. Smith and V. Yakhot, Phys. Rev. Lett. **71**, 352 (1993).
[8] D. Biskamp and H. Welter, Phys. Fluids B **1**, 1964 (1989).
[9] V. D. Larichev and J. C. McWilliams, Phys. Fluids A **3**, 938 (1991).
[10] N. Kukharkin, S. A. Orszag, and V. Yakhot, Phys. Rev. Lett. **75**, 2486 (1995).
[11] D. Biskamp, E. Schwarz, and J. F. Drake, Phys. Rev. Lett. **76**, 1264 (1996).
[12] A. Celani, R. Prandi, and G. Boffetta, Europhys. Lett. **41**, 13 (1998).
[13] See, e.g., D. Biskamp, E. Schwarz, and A. Zeiler, Phys. Plasmas **5**, 2485 (1998).
[14] S. V. Bulanov, M. Lontano, T. Zh. Esirkepov, F. Pegoraro, and A. M. Pukhov, Phys. Rev. Lett. **76**, 3562 (1996).
[15] S. V. Bulanov, T. Zh. Esirkepov, M. Lontano, and F. Pegoraro, Plasma Phys. Rep. **23**, 660 (1997).
[16] S. Galtier, H. Politano, and A. Pouquet, Phys. Rev. Lett. **79**, 2807 (1997).
[17] P. S. Iroshnikov, Sov. Astron. **7**, 566 (1964).
[18] R. H. Kraichnan, Phys. Fluids **8**, 1385 (1965).
[19] J. F. Drake, D. Biskamp, and A. Zeiler, Geophys. Res. Lett. **24**, 2921 (1997).
[20] Z. S. She, S. Chen, G. Doolen, R. H. Kraichnan, and S. A. Orszag, Phys. Rev. Lett. **70**, 3251 (1993).
[21] D. Biskamp, E. Schwarz, and A. Celani, Phys. Rev. Lett. **81**, 4855 (1998).